Melting Points—The Key to the Anti-Evaporative Effect of the Tear Film Wax Esters

Antti H. Rantamäki,[1] Susanne K. Wiedmer,[2] and Juha M. Holopainen[1]

[1]Helsinki Eye Lab, Department of Ophthalmology, University of Helsinki, Helsinki, Finland
[2]Department of Chemistry, University of Helsinki, Helsinki, Finland

Corresponding author: Juha M. Holopainen, Helsinki Eye Lab, Department of Ophthalmology, University of Helsinki, PO Box 220, 00029 HUS, Finland; juha.holopainen@hus.fi.

Submitted: May 14, 2013
Accepted: June 24, 2013

Citation: Rantamäki AH, Wiedmer SK, Holopainen JM. Melting points—the key to the anti-evaporative effect of the tear film wax esters. *Invest Ophthalmol Vis Sci*. 2013;54:5211–5217. DOI:10.1167/iovs.13-12408

Purpose. We examined in vitro the evaporation-retarding effect of wax esters (WEs). The WEs resembled closely the most abundant WE species in meibum.

Methods. A custom-built system was used to measure the evaporation rates through WE layers applied to the air–water interface at 35°C and, as a reference, at 30°C and 41°C. Additionally, the melting points of the WEs were determined. The organization and stability of the WE layers were assessed using Brewster angle microscopy (BAM) and Langmuir film experiments, respectively.

Results. Four of 19 WEs retarded evaporation at 35°C: behenyl palmitoleate (BP), behenyl oleate (BO), behenyl linoleate (BLN), and behenyl linolenate (BLNN) decreased evaporation by 20% to 40%. BP was the most effective evaporation retardant. At 30°C the most effective retardants were BLN and BLNN decreasing evaporation by ~50%, whereas BP and BO decreased evaporation by only 5% to 10%. At 41°C, each lipid decreased evaporation by only 2% to 4%. The evaporation-retardant WEs all melted within 2°C of physiological temperature. BAM images showed that the evaporation-retardant WE layers spread somewhat uniformly and possibly exhibited areas of condensed lipid. The isotherms suggested that WE layers were surface pressure tolerant but unstable under compression–relaxation cycles.

Conclusions. The evaporation-retarding effect is dependent on the physicochemical properties of the WEs at given temperature, and therefore, the effect most likely arises from a certain phase of the WE layer. However, WEs as such are poor surfactants and need to be accompanied by polar lipids to form stable lipid layers.

Keywords: dry eye, evaporation, wax ester

Ocular surface-protecting tear film can be divided into three qualitatively different layers: a viscous network of mucins lining the epithelium; an overlapping aqueous layer containing dissolved proteins, salts, and metabolites; and a tear film lipid layer (TFLL) at the air-tear interface, consisting of myriad lipids, both polar and nonpolar.[1–6]

TFLL allegedly is an effective evaporation retardant in in vivo tear film,[7–10] whereas based on in vitro experiments, the evaporation-retarding effect is disputable.[11–15] Meibum, for instance, is a poor evaporation retardant in vitro (6%–8% reduction in evaporation rate).[12,14] The molecular level knowledge of efficient evaporation-retarding lipid layers, such as fatty alcohols or fatty acids,[16–18] and the current opinion on TFLL composition are contradictory.[1–6] This suggests that there are three plausible options regarding the retardation of evaporation of tear film: (1) the evaporation-retarding effect is based on a certain multilayered organization of the lipid layer as proposed previously[19]; (2) the lipid layer is not the sole structure responsible for the retardation of evaporation, but specific protein interactions are needed for this process; or (3) water evaporation from the ocular surface is not at all controlled by lipids and the lipid layer has other functions.[14,20]

In our previous study, we investigated in vitro TFLL-like lipid layers and concluded that such compositions did not retard evaporation.[13] Only a certain wax ester (WE) investigated in that study, behenyl oleate (BO), retarded evaporation but only when 10% (mol/mol) or less of the non–evaporation-retarding lipid was present. We concluded that the condensed phase of the lipid layer, such as the one formed by BO, is vital for the evaporation-retarding effect of the lipid layer. In the present study, we investigated in more detail a series of other WEs with varying chain lengths and degrees of saturation and their abilities to retard evaporation by using the same system as in the previous study. We hypothesized that this effect can be deduced from simple physicochemical properties of WEs. Brewster angle microscopy (BAM) was used to investigate the organization of the WEs at the air–water interface, and Langmuir balance measurements were made to reveal details of the surfactant properties of the WE layers.

Methods

Lipids

WEs were acquired from Nu-Check-Prep (Elysian, MN), except for BO, which was from Sigma-Aldrich (St. Louis, MO). Behenyl alcohol (BAl) was purchased from Sigma-Aldrich.

Melting Point Determination

WE melting points were measured using a melting point apparatus (Stuart SMP10; Bibby Scientific Ltd., Staffordshire,

UK). The temperature was ramped 2°C/min until the melting point was reached. The temperature accuracy of the apparatus at 20°C was ±1°C. The melting point of each solid state WE (at ~22°C) was measured four times.

Evaporation Rate Experiments

The evaporation experiments were performed mainly as described in our previous study.[13] In short, 500 nmol of lipid was applied to the air–water interface, and the evaporation rate through the lipid layer was determined based on the changed mass of the subphase. Measurements were made at near-physiological temperature, and the average subphase temperature was 35.4°C ± 0.6°C when the air–water interface was either pure or covered with a nonevaporation-retardant lipid. The retardant WEs had a tendency to raise the subphase temperature due to the less efficient heat dissipation caused by the slower evaporation. When the evaporation-retardant WEs were present, the average temperature was 36.4°C ± 0.6°C. For reference, evaporation rates were measured for selected lipids using subphase temperatures, which were ~5°C below and above the physiological temperature. Average temperatures were 29.9°C ± 0.4°C (30.9°C ± 0.7°C with evaporation-retardant WEs) and 41.0°C ± 0.4°C (41.4°C ± 0.6°C with evaporation-retardant WEs).

At 35°C, the relative humidity during the measurement varied from 27% to 38% when the air–water interface was either pure or covered with nonevaporation-retardant WEs and from 22% to 29% when the interface was covered with retardant WEs. This variation was caused by the nonairtight assembly of the apparatus. At 30°C, the range for pure interface and all WEs was from 14% to 30% and at 41°C from 32% to 38%.

The evaporation rate through each lipid layer was measured at least three times for lipid layers that retarded evaporation and two times for lipid layers that did not retard evaporation. A one-way ANOVA method was used for comparison between the evaporation rates generated by the pure interface and those generated by the lipid-covered air–water interfaces. A P value of <0.05 was considered significant.

Brewster Angle Microscopy

MicroBAM (KSV NIMA, Helsinki, Finland) and Mini Trough (KSV, Helsinki, Finland) units were used to assess the spreading and lateral organization of selected WE layers at 35°C. Lignoceryl lignocerate (LL) and lauryl oleate (LO) represented solid state and liquid state WEs, respectively, whereas BO, behenyl palmitoleate (PB), behenyl linoleate (BLN), and behenyl linolenate (BLNN) were selected because they retard evaporation and are close to their melted state at 35°C. The lipid was applied to the surface as described in the evaporation rate experiments in order to replicate the conditions. Instead of 500 nmol, 1000 nmol of lauryl oleate (LO) was used for visualization purposes to reveal the white-shaded aggregation (the surface pressures produced by 500 nmol and 1000 nmol were equal). The lipid layers were observed over a period of 15 minutes after spreading. Each lipid layer was imaged twice.

Langmuir Film Experiments

A Mini trough (KSV) was used to record compression isotherms for selected WE layers. WEs were selected based on their melting points and ability to retard evaporation. BL represented solid state WEs, and arachidyl oleate (AO) and LO liquid state WEs; whereas BO, BL, BLN, and BLNN were selected because they retard evaporation and are close to their melted state at 35°C. The lipid in 10 mM chloroform solution was applied to the surface of the PBS subphase. The lipid layer was compressed and relaxed at a speed of 10 mm/min 5 times until either a 45 mN/m surface pressure was achieved or the barrier reached the stopper. Only subtle changes were observed between the fourth and fifth compression–relaxation cycles. The number of cycles was limited by the evaporation of the subphase during the measurement. The amount of lipid was adjusted so that the maximum compression could be achieved on the fifth cycle, starting from ~0 mN/m. The isotherms for each lipid layer were recorded twice to ensure good repeatability of results.

Results

Melting Point Determination

At room temperature, the WEs had three appearances: liquid, powder, and plastic wax. As expected, the measured melting points (Table) clearly followed the dependence on lengths and saturation of the carbon chains, LL having the highest and behenyl arachidonate the lowest melting point of all WEs measured.

Evaporation Rate Experiments

Evaporation-retarding effects of WEs are presented in the Table as positive/negative comparison; quantitative values are given in Supplementary Table S1. Figure 1 presents the percentages of decrease in evaporation rates relative to the evaporation rates from the pure air–water interface. BAl was used as the positive (evaporation-retarding) control. Results are given as a value ± propagation of uncertainty (based on evaporation rate standard errors). At 35°C, BO, BP, BLN, and BLNN were the WEs that retarded evaporation. BP was the strongest evaporation retardant, decreasing evaporation rate by 39% ± 3%. BO and BLN shared similar evaporation-retarding effects (30% ± 2% and 27% ± 2%, respectively), whereas BLNN was the weakest evaporation retardant (20% ± 1%). At 30°C, BLN and BLNN were clearly stronger retardants than BP and BO, decreasing evaporation by 51% ± 10%, 52% ± 4%, 12% ± 1%, and 5.2% ± 0.2%, respectively. In addition, AO decreased evaporation by 16% ± 1%. At 41°C, BO, BP, BLN, BLNN, and AO decreased evaporation by only 2.3% to 3.6%. BAl, the positive control, decreased the evaporation by 62% ± 6% at 35°C, 41 ± 3% at 30°C, and 63% ± 1% at 41°C. Relative to the pure air–water interface, the evaporation rates through evaporation-retarding WE layers were statistically significant ($P < 0.05$), excluding BO at 30°C.

The surface pressures produced by the WEs during evaporation experiments at 35°C ranged from 0.5 to 6.5 mN/m. LO produced the highest and behenyl arachidate and LL the lowest surface pressures. Generally, the monounsaturated WEs, which have melting points lower than 35°C (i.e., lauryl, myristyl, and palmityl oleates) produced the highest surface pressures, whereas the WEs with melting points clearly higher than 35°C, starting from behenyl laurate (BL) resulted in the lowest surface pressures. The surface pressures produced by BO, BP, BLN, and BLNN at 35°C ranged from 2.4 to 4.9 mN/m. At 30°C and 41°C, the surface pressures produced by these WEs were somewhat lower, ranging from 0.4 to 2.7 mN/m and from 2.1 to 2.7 mN/m, respectively. As an exception, the surface pressure produced by AO remained relatively stable at differing temperatures, ranging only from 3.4 to 4.1 mN/m.

Brewster Angle Microscopy

BAM images are shown in Figure 2. The positive control, BAl, formed a uniformly spread layer, which was in condensed

TABLE. Wax Esters, Structures, Melting Points (±1°C), and Evaporation-Retarding Effects at 35°C and as a Reference at 30°C and 41°C for Selected Wax Esters

Wax Ester	Structure, FAl/FA	MP, °C	$RE_{35°C}$	$RE_{30°C}$	$RE_{41°C}$
Linolenyl oleate*	18:3/18:1	<22	–		
Lauryl oleate (LO)*	12:0/18:1	<22	–		
Myristyl oleate*	14:0/18:1	<22	–		
Palmityl oleate*	16:0/18:1	<22	–		
Stearyl oleate*	18:0/18:1	<22	–		
Behenyl arachidonate*	22:0/20:4	27	–		
Arachidyl oleate (AO)†	20:0/18:1	33	–	++	–
Behenyl linolenate (BLNN)†	22:0/18:3	36	+	+++	–
Behenyl linoleate (BLN)†	22:0/18:2	37	++	+++	–
Behenyl oleate (BO)†	22:0/18:1	38	++	–	–
Behenyl palmitoleate (BP)†	22:0/16:1	38	+++	+	–
Behenyl laurate (BL)‡	22:0/12:0	54	–		
Behenyl myristate‡	22:0/14:0	58	–		
Behenyl palmitate‡	22:0/16:0	63	–		
Behenyl stearate‡	22:0/18:0	67	–		
Behenyl arachidate‡	22:0/20:0	73	–		
Behenyl behenate‡	22:0/22:0	75	–		
Behenyl lignocerate‡	22:0/24:0	77	–		
Lignoceryl lignocerate (LL)‡	24:0/24:0	79	–		

The positive/negative comparison is based on the evaporation retarding effects within each temperature point. Negative sign designates an evaporation rate decrease of <10% relative to the blank value. FA, fatty acid; FAl, fatty alcohol; MP, melting point; RE, retardation of evaporation.

* Low MP.

† MP in near-physiologic temperatures.

‡ High MP.

phase as implied by the gray shade barely visible in the left lower-exposure image. Images of the BO, BLN, and BLNN layers and the accompanying surface pressure information (3.3–3.7 mN/m) suggest that the lipid layer covered the entire surface. The images also show a large number of white-shaded aggregates (in constant parallel movement during imaging) mixed with the black-shaded liquid phase lipid. The BP layer spread rapidly and resulted in a surface pressure (4.3 mN/m) similar to the other evaporation-retardant WEs but appeared more layered (white shades) and almost stagnant. Additionally, the extensive amount of gray shading implies that the layer may be partly in condensed phase. The liquid state LO showed less aggregation (despite the fact that twice the amount of lipid was used here) and higher surface pressure than the other layers (5.9 mN/m). The LL layer image showed, as expected, high-level aggregation of the lipid due to the solid state of the bulk lipid. Also, the close-to-zero surface pressure (0.2 mN/m) implies that no spreading took place.

Compression Isotherms

The recorded compression isotherms are shown in Figure 3. The relatively nonpolar/hydrophobic WEs needed several compression–relaxation cycles to achieve the final organization. The WE layers shared several common properties: they reached very small molecular areas and surprisingly high surface pressures during compression; the compressibility of the WE layers decreased gradually during the consecutive compression–relaxation cycles, as suggested by the steepness of the isotherms (Fig. 3, inset); the liftoff area of the isotherms moved to smaller molecular areas; and the isotherms suggest somewhat large hysteresis by relaxation. The liquid state WEs AO and LO had higher compressibilities than the more solid WEs and showed less hysteresis at higher surface pressures. The evaporation retardant BO, BP, BLN, and BLNN showed very similar behavior when compared to each other. The solid state BL produced an extraordinary spike-like isotherm suggesting close-to-zero compressibility and poor spreading.

DISCUSSION

The purpose of this study was to investigate in more detail the evaporation-retarding effect of WEs, because they are a major lipid component in TFLL. In meibum, the most abundant WEs are based on oleic (~75%), or palmitoleic acid (~8%) and 24:0, 25:0, 26:0 and 27:0 branched fatty alcohols.[3,20,21] For this study, the WEs were selected as close as possible to those found in meibum. We endeavored to reveal more details about the evaporation-retarding effect and the physical behavior of these somewhat hydrophobic molecules at the air–water interface, using mainly Langmuir film techniques.

It must be mentioned that studying WEs using the Langmuir film techniques is challenging, because their hydrophobic characteristics lead to aggregation at the air–water interface. Therefore, the concentration and volume of the liquid in which WEs are applied to the surface affect the liftoff area of the isotherms. Second, the profiles of the WE isotherms are not as repeatable as with phospholipids due to the low compression stability of the layers. Therefore, the results must be interpreted cautiously.

To begin with, we measured the melting points of WEs because, surprisingly, this data could not be found from the literature. Based on the melting points, the WEs were grouped into three categories: those that have their melting points much lower than the physiological temperature, those that have their melting points close the physiological temperature, and those that have extremely high melting points (Table).

We measured the evaporation rates at the near-physiological temperature of 35°C and found out that four WEs were evaporation retardant (Fig. 1). BP, BLN, and BLNN, in addition to BO discovered in our previous study[13] decreased evaporation rates by 20% to 40%. A common factor for these lipids was that they melted within 2°C of the physiological temperature. By visual inspection alone we noticed clear differences in the spreading of the lipids. The saturated long-chain WEs spread poorly, forming raft-like aggregates at the air–water interface,

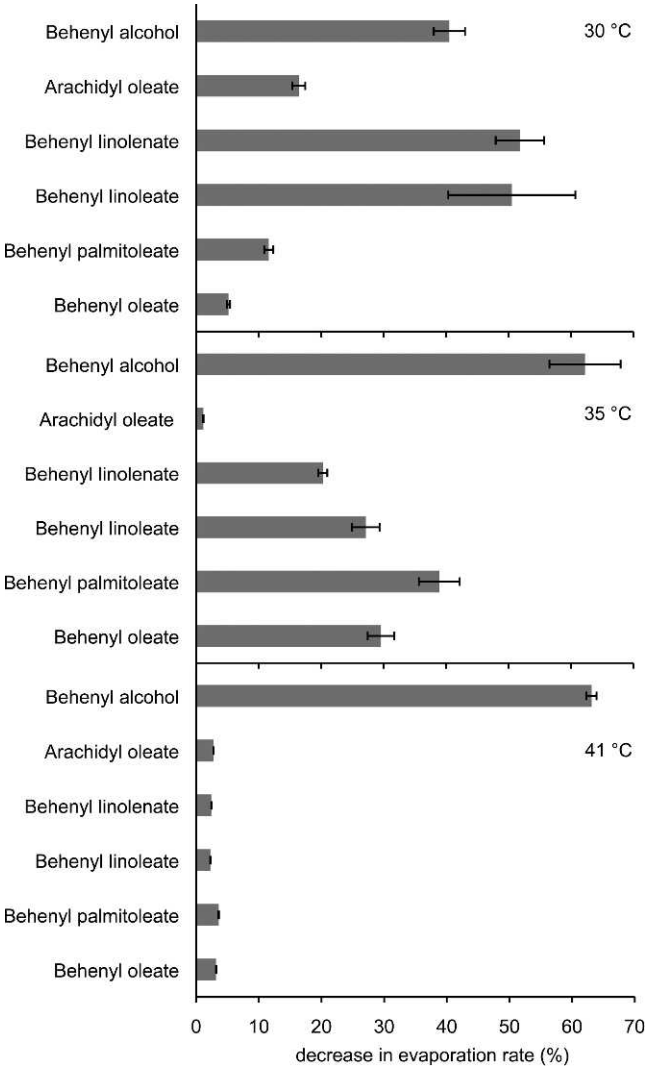

FIGURE 1. Percentage decrease in evaporation rates relative to the evaporation rate from pure air–water interface at 30°C, 35°C, and 41°C. Behenyl alcohol was used as the positive control.

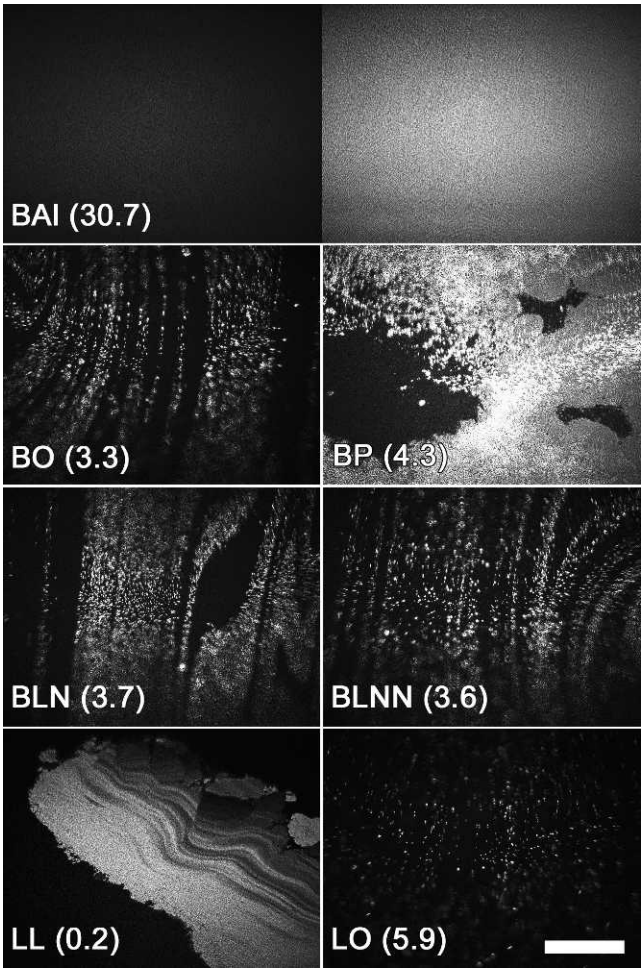

FIGURE 2. BAM images of selected WE layers at 35°C. The exposure settings are the same in each image except for the right-hand image of BAI, which was captured using higher exposure, and the LL image, which was captured using lower exposure, to reveal more details. Surface pressures are given in parenthesis as mN/m. *Scale bar*: 1000 μm. BAI, behenyl alcohol; BLN, behenyl linoleate; BLNN, behenyl linolenate; BO, behenyl oleate; BP, behenyl palmitoleate; LL, lignoceryl lignocerate; LO, lauryl oleate.

whereas shorter-chain and unsaturated WEs spread more uniformly.

The observations above suggested that the differences in the evaporation-retarding effects of WEs were caused by certain peculiar physical properties of WEs, when they are very close to their solid–liquid phase transition. More simply, if the WEs are in their solid state, a large area of the interface is not covered by lipid and the lipid rafts float like icebergs on the sea. Similarly, when WEs are in a very fluid-like state, the extensive wobbling motion of lipids allows for a large free-volume to accumulate within the lipid membrane, and this allows the water molecules to travel through the WE membrane.[22] At close to their melting point, WEs form a structure, tentatively reminiscent of percolated or soft monolayers,[23] which retards evaporation. This is distinctive behavior, as the evaporation-retarding effect is not related to the melting point for the more typical retardants such as BAI (melting point of 71°C ± 1°C).[24] In these layers the evaporation-retarding effect is achieved by very tight packing of the acyl chains, with exceedingly low free volume within the lipid layer.

As the evaporation-retarding effect was obviously related to the melting point, we also measured the evaporation rates through BO, BP, BLN, and BLNN layers at 30°C and 41°C. The purpose was to discover whether these lipids still retarded evaporation when they were more clearly in solid state at 30°C or in liquid state at 41°C. At 30°C BLN and BLNN, having the lowest melting points of the four WEs, decreased evaporation by ~50%, whereas BP and BO retarded evaporation by only 5% to 10%. At 41°C, the decrease in evaporation was only 2% to 4%, when all the WEs were in liquid state. In summary, the data suggest that the melting point of the lipid has to be at or just above the interfacial temperature for the retardation of evaporation to occur.

To further test this theory of melting point dependency, we measured the evaporation-retarding effect of AO also at 30°C and 41°C. AO was selected because it melts at 33°C ± 1°C and, therefore, should retard evaporation at 30°C, based on our theory. As expected, this indeed was the case. AO decreased the evaporation rate by 16% ± 1%, but it did not retard evaporation at 41°C as expected. The evaporation-retarding

Investigative Ophthalmology & Visual Science

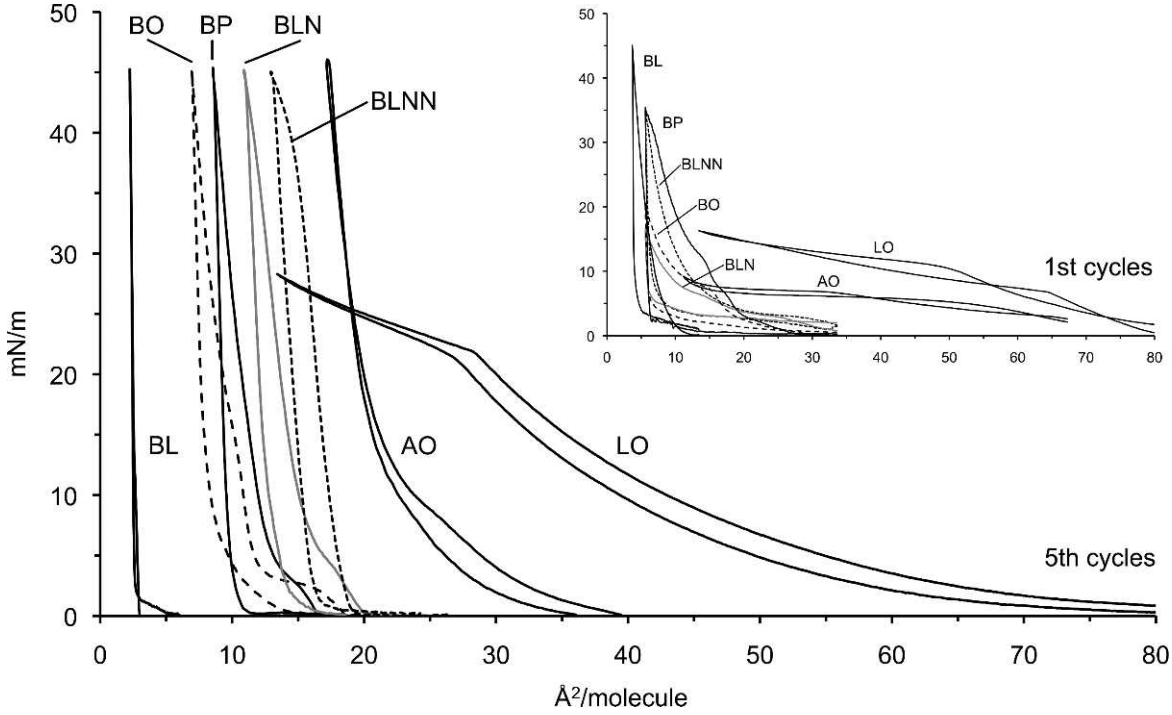

FIGURE 3. Compression isotherms for selected WEs after five compression–relaxation cycles at 35°C. *Inset* shows the first cycle for each WE layer. AO, arachidyl oleate; BL, behenyl laurate; BLN, behenyl linoleate; BLNN, behenyl linolenate; BO, behenyl oleate; BP, behenyl palmitoleate; LO, lauryl oleate.

effect was noticeably smaller than those of BLN and BLNN and only ~5% larger than that of BP.

At 35°C, the differing spreading behavior of WE species was observed using BAM (Fig. 2). Long-chain saturated LL formed thick three-dimensional aggregates at the interface, whereas short-chain LO spread more uniformly, showing only few small aggregates. Based on the BAM images alone, we cannot assume that the black areas are covered with a lipid layer; however, the higher surface pressure produced by LO suggests that it is more uniformly spread than LL. The similar aggregate formation and surface pressures of BO, BLNN, and BLN accompanied with the similar evaporation-retarding effect imply that these WE layers were in the same phase. BP also spread uniformly when applied to the interface but also formed larger areas of layered/aggregated lipid layer. The somewhat stagnant appearance of BP also reminded us of a phase that is condensed or gel-like compared to the more liquid BO, BLN, and BLNN layers. As a reference, Figure 2 (upper panel) shows a uniformly spread BAl layer. The gray shading, presented more clearly in the high-exposure image on the right-hand side, indicates that the layer is in a condensed phase. The effective evaporation-retarding effect of BAl is caused by the small cross-sectional area of the molecule (small polar head group and only one hydrophobic alkyl chain), which enables close packing of the molecules.

Based on the BAM images, it seems likely that the evaporation-retarding effect for these four WEs is the result of the condensed-like phase existing at the proximity of the liquid-condensed phase transition, as hypothesized above. BP seems somewhat more condensed than the BO, BLN, and BLNN layers; hence, the more efficient evaporation-retarding effect of the BP layer. The WEs possibly organize at the air–water interface so that the carboxyl group is in the aqueous phase and the alcohol and acyl chains point toward the air in a V-shaped manner.[25] However, aggregation or stacking of layered structures is also expected, as 500 nmol of WE spread uniformly results here as a mean area of ~9 Å^2/molecule, whereas the minimum molecular area for a fatty alcohol is ~20 Å^2. Therefore, the approximated thickness of these layers is <100 nm, depending on the minimum mean molecular area occupied by the WEs. This is the same order of magnitude as the in vivo thickness of TFLL.[26]

The isotherms indicate that the selected WE layers share common properties (Fig. 3). The transfer of the liftoff area is simply explained by increased aggregation, that is, excess WEs are pushed out of the interface to form a new overlaying layer, either as an organized structure or as bulky three-dimensional aggregates. Consecutive compression cycles cause the WE layer to aggregate more, and because of the hydrophobic nature, it is energetically more favorable for the "excess" molecules not to return to the interface on relaxation. This poor respreading shows as large hysteresis observed in the isotherms. The decrease in compressibility instead results in steeper isotherm profiles when compared to the first cycles. Finally, the isotherms also suggest that WEs at the air–water interface take a somewhat organized lateral structure since the layers are tolerant to high surface pressures without collapsing.

As expected, the liquid state LO and AO were the most compressible of the WEs tested. They also showed less hysteresis, especially at higher surface pressures. The kinks at ~8 mN/m for AO and ~23 mN/m for LO also suggest phase transition, but the phase transitional behavior of these WE layers is beyond the scope of this study, as the evaporation-retarding effect existed already at lower surface pressures (<5 mN/m) than where the potential phase transitions took place. In contrast, solid state BL at the other extreme has a spike-like isotherm profile. The profile is easily explained by visual inspection of the lipid layer, or moreover a lipid raft, during compression. By the first compression, BL behaved somewhat similarly to the other WE layers, but by relaxation, no spreading took place due to the solid state of the lipid. BL

stayed floating as a vast raft in the middle of the trough. Therefore, during consecutive compression–relaxation cycles the changes in surface pressure took place during very minimal movement of the Langmuir balance barriers due to the close-to-zero compressibility of the raft. The surfactant properties of evaporation-retardant WEs located well between the solid state BL and liquid state AO, as expected based on the melting point of these four evaporation-retardant lipids. However, based on the isotherms it is challenging to draw any further conclusions about the structural properties of the lipid layers that induce the evaporation-retardant nature of the WE layer. It is clear that these four retardant layers have very similar surfactant properties and, therefore, most likely very similar structures. Overall, the Langmuir film experiments unveiled the poor compression–expansion behavior of the WE layers.

The dependency between the physical state of the WE layer at given temperatures and the ability to retard evaporation may partially explain the aging-related changes in the meibum composition and therefore in the stability of the tear film.[27,28] One may speculate that because of the changes in WE structures, such as changed degree of saturation and branching of the carbon chains, the order and melting temperature of the TFLL decrease and lead to a reduced ability to retard evaporation. Therefore it is possible that the infant TFLL retards evaporation more effectively than an adult TFLL, which would also explain the lower blinking frequency of the infants.

In summary, we have shown here that only certain WEs retard evaporation at physiological temperatures. The ability to retard evaporation is dependent on the physical properties of the WEs at a given temperature. The evaporation-retarding effect may be explained by formation of a specific condensed-like phase of the WE layer, which exists at the proximity of the solid–liquid phase transition. Under conditions of consecutive compression–relaxation cycles, the buildup of multilayered or aggregated WE structures continues until a pressure-tolerant WE layer is formed. Despite the high surface pressure tolerance, WEs are missing the main hallmarks of a stable lipid layer. They organize very slowly into a layer form, prefer aggregation over uniform spreading, are incompressible, and finally, create lipid layers that are unstable in a dynamic environment. Therefore, they need to be accompanied by more efficient surfactants such as polar phospholipids. As emphasized in our previous studies, phospholipids, such as phosphatidylcholine and sphingomyelin, are prerequisites for the spreading and controlled function of TFLL-like lipid layers.[4,29–31] If such an evaporation-retardant TFLL-like lipid layer composed of nonpolar and polar lipids exists, WEs most likely play a major role in that structure.

Acknowledgments

This study was supported by the Finnish Eye Foundation, the Academy of Finland, the Sigrid Juselius Foundation, and the Magnus Ehrnrooth foundation.

Disclosure: **A.H. Rantamäki**, None; **S.K. Wiedmer**, None; **J.M. Holopainen**, Croma Pharma Austria (C)

References

1. Bron AJ, Tiffany JM, Gouveia SM, Yokoi N, Voon LW. Functional aspects of the tear film lipid layer. *Exp Eye Res*. 2004;78:347–360.
2. Rantamäki AH, Telenius J, Koivuniemi A, Vattulainen I, Holopainen JM. Lessons from the biophysics of interfaces: lung surfactant and tear fluid. *Prog Retin Eye Res*. 2011;30:204–215.
3. Butovich IA. Lipidomics of human meibomian gland secretions: chemistry, biophysics, and physiological role of meibomian lipids. *Prog Lipid Res*. 2011;50:278–301.
4. Rantamäki AH, Seppänen-Laakso T, Oresic M, Jauhiainen M, Holopainen JM. Human tear fluid lipidome: from composition to function. *PLoS One*. 2011;6:e19553.
5. Saville JT, Zhao Z, Willcox MD, Ariyavidana MA, Blanksby SJ, Mitchell TW. Identification of phospholipids in human meibum by nano-electrospray ionisation tandem mass spectrometry. *Exp Eye Res*. 2011;92:238–240.
6. Dean AW, Glasgow BJ. Mass spectrometric identification of phospholipids in human tears and tear lipocalin. *Invest Ophthalmol Vis Sci*. 2012;53:1773–1782.
7. Mishima S, Maurice DM. The oily layer of the tear film and evaporation from the corneal surface. *Exp Eye Res*. 1961;1:39–45.
8. Iwata S, Lemp MA, Holly FJ, Dohlman CH. Evaporation rate of water from the precorneal tear film and cornea in the rabbit. *Invest Ophthalmol*. 1969;8:613–619.
9. Craig JP, Tomlinson A. Importance of the lipid layer in human tear film stability and evaporation. *Optom Vis Sci*. 1997;74:8–13.
10. Craig JP, Singh I, Tomlinson A, Morgan PB, Efron N. The role of tear physiology in ocular surface temperature. *Eye*. 2000;14:635–641.
11. Borchman D, Foulks GN, Yappert MC, Mathews J, Leake K, Bell J. Factors affecting evaporation rates of tear film components measured in vitro. *Eye Contact Lens*. 2009;35:32–37.
12. Herok GH, Mudgil P, Millar TJ. The effect of meibomian lipids and tear proteins on evaporation rate under controlled in vitro conditions. *Curr Eye Res*. 2009;34:589–597.
13. Rantamäki AH, Javanainen M, Vattulainen I, Holopainen JM. Do lipids retard the evaporation of the tear fluid? *Invest Ophthalmol Vis Sci*. 2012;53:6442–6447.
14. Cerretani CF, Ho NH, Radke CJ. Water-evaporation reduction by duplex films: Application to the human tear film. *Adv Colloid Interface Sci*.
15. Borchman D, Yappert MC, Milliner SE, et al. ^{13}C and ^{1}H NMR ester region resonance assignments and the composition of human infant and child meibum. *Exp Eye Res*. 2013;112:151–159.
16. Rosano HL, La Mer VK. The rate of evaporation of water through monolayers of esters, acids and alcohols. *J Phys Chem*. 1956;60:348–353.
17. La Mer VK, Healy TW. Evaporation of water: Its retardation by monolayers: Spreading a monomolecular film on the surface is a tested and economical means of reducing water loss. *Science*. 1965;148:36–42.
18. Barnes GT. The potential for monolayers to reduce the evaporation of water from large water storages. *Agric Water Manage*. 2008;95:339–353.
19. McCulley JP, Shine W. A compositional based model for the tear film lipid layer. *Trans Am Ophthalmol Soc*. 1997;95:79–88; discussion 88-93.
20. Butovich IA, Arciniega JC, Lu H, Molai M. Evaluation and quantitation of intact wax esters of human meibum by gas-liquid chromatography-ion trap mass spectrometry. *Invest Ophthalmol Vis Sci*. 2012;53:3766–3781.
21. Nicolaides N, Kaitaranta JK, Rawdah TN, Macy JI, Boswell FM, 3rd, Smith RE. Meibomian gland studies: comparison of steer and human lipids. *Invest Ophthalmol Vis Sci*. 1981;20:522–536.
22. Sane P, Salonen E, Falck E, et al. Probing biomembranes with positrons. *J Phys Chem B*. 2009;113:1810–1812.
23. Mouritsen OG, Zuckermann MJ. Softening of lipid bilayers. *Eur Biophys J*. 1985;12:75–86.

24. Physical constants of organic compounds. In: H.M. Haynes, TJ Bruno and DR Lide, eds. *Handbook of Chemistry and Physics, Internet version*. Boca Raton, FL: CRC Press; 2013;236.
25. Adam NK. The structure of surface films. Part XIV. Some esters of fatty acids. Evidence of flexibility in the long chains. *Proc R Soc Lond A*. 1930;126:366–372.
26. King-Smith PE, Hinel EA, Nichols JJ. Application of a novel interferometric method to investigate the relation between lipid layer thickness and tear film thinning. *Invest Ophthalmol Vis Sci*. 2010;51:2418–2423.
27. Borchman D, Foulks GN, Yappert MC, et al. Physical changes in human meibum with age as measured by infrared spectroscopy. *Ophthalmic Res*. 2010;44:34–42.
28. Borchman D, Foulks GN, Yappert MC, Milliner SE. Changes in human meibum lipid composition with age using nuclear magnetic resonance spectroscopy. *Invest Ophthalmol Vis Sci*. 2012;53:475–482.
29. Kulovesi P, Telenius J, Koivuniemi A, et al. Molecular organization of the tear fluid lipid layer. *Biophys J*. 2010;99:2559–2567.
30. Kulovesi P, Telenius J, Koivuniemi A, Brezesinski G, Vattulainen I, Holopainen JM. The impact of lipid composition on the stability of the tear fluid lipid layer. *Soft Matter*. 2012;8:5826–5834.
31. Telenius J, Koivuniemi A, Kulovesi P, Holopainen JM, Vattulainen I. Role of neutral lipids in tear fluid lipid layer: Coarse-grained simulation study. *Langmuir*. 2012;28:17092–17100.

Investigative Ophthalmology & Visual Science